# Supplementary material: Unveiling the Microscopic Origins and Thermoelectric Performance of full-Heusler compounds $K_2RbSb$ and $Rb_2KSb$

Peipei Liu,[1] Yinchang Zhao,[1,*] Jun Ni,[2,3] and Zhenhong Dai[1,†]

[1]*Department of Physics, Yantai University, Yantai 264005, People's Republic of China*

[2]*State Key Laboratory of Low-Dimensional Quantum Physics, Department of Physics, Tsinghua University, Beijing 100084, People's Republic of China*

[3]*Frontier Science Center for Quantum Information, Beijing 100084, People's Republic of China*

(Dated: December 31, 2024)

PACS numbers: 65.40.-b, 66.70.-f, 63.20.-e, 72.20.-i

Keywords: full-Heusler compound, first-principles calculation, transport properties, thermoelectric properties

## A. Supplementary Calculation Detail.

### *1. Thermal Transport*

In our calculations, the HA IFCs were captured using the finite displacement method. Specifically, we included all HA IFCs within the supercell and used a displacement distance of $\triangle$x=0.01 Å. Additionally, non-harmonic IFCs were trained based on CSLD techniques. To obtain the displacement and force data sets required for nonharmonic (cubic and quartic) IFCs, we used 4000-step ab initio molecular dynamics (AIMD) simulations, capturing 80 Snapshots at 300 K with a time step of 2 fs. On this basis, we added a random displacement of 0.1 Å to each atom of the 80 snapshots and obtained 80 quasirandom configurations, then derived anharmonic IFCs .

The group velocity of phonon mode $\mathbf{qj}$ is given by

$$v_{\mathbf{qj}} = \frac{\partial w_{\mathbf{qj}}}{\partial \mathbf{q}} \tag{S1}$$

The mode Grüneisen parameter, defined as

$$\gamma_{\mathbf{qj}} = -\frac{\partial \log w_{\mathbf{qj}}}{\partial \log V} \tag{S2}$$

### *2. Electron Transport*

For electron transport properties, five scattering mechanisms were considered, including ADP, POP, IMP, PIE, and MFP scattering. These were calculated from first-principles-derived material parameters. In particular, The differential scattering rate from state $|n\mathbf{k}\rangle$ to state $|m\mathbf{k}+\mathbf{q}\rangle$ is calculated using Fermi's golden rule as

$$\widetilde{\tau}^{-1}_{n\mathbf{k}\to m\mathbf{k}+\mathbf{q}} = \frac{2\pi}{\hbar} \mid g_{nm}(\mathbf{k},\mathbf{q}) \mid^2 \delta(\varepsilon_{n\mathbf{k}} - \varepsilon_{m\mathbf{k}+\mathbf{q}}) \tag{S3}$$

where $\varepsilon_{n\mathbf{k}}$ is the energy of state $|n\mathbf{k}\rangle$, and $g_{nm}(\mathbf{k},\mathbf{q})$ is the matrix element for scattering from state $|n\mathbf{k}\rangle$ into $|m\mathbf{k}+\mathbf{q}\rangle$ state.

The acoustic deformation potential matrix element is given by

$$g_{nm}^{ADP}(\mathbf{k},\mathbf{q}) = \sqrt{k_B T} \sum_{\mathbf{G}\neq-\mathbf{q}} \left[ \frac{\widetilde{\mathbf{D}}_{nk} : \hat{\mathbf{S}}_l}{c_{l\sqrt{\rho}}} + \frac{\widetilde{\mathbf{D}}_{nk} : \hat{\mathbf{S}}_{t_1}}{c_{t_1\sqrt{\rho}}} + \frac{\widetilde{\mathbf{D}}_{nk} : \hat{\mathbf{S}}_{t_2}}{c_{t_2\sqrt{\rho}}} \right] \left\langle m\mathbf{k}+\mathbf{q} \mid e^{i(\mathbf{q}+\mathbf{G})\cdot\mathbf{r}} \mid n\mathbf{k} \right\rangle \tag{S4}$$

where $\widetilde{\mathbf{D}}_{nk} = \mathbf{D}_{nk} + \mathrm{v}_{nk} \otimes \mathrm{v}_{nk}$ in which $\mathbf{D}_{nk}$ is the rank 2 deformation potential tensor, $\hat{\mathbf{S}} = \hat{\mathbf{q}} \otimes \hat{\mathbf{u}}$ is the unit strain associated with an acoustic mode, $\mathbf{u}$ is the unit vector of phonon polarization, and the subscripts $l$, $t_1$ and $t_2$ indicate properties belonging to the longitudinal and transverse modes.

The piezoelectric differential scattering rate is given by

$$g_{nm}^{PIE}(\mathbf{k},\mathbf{q}) = \sqrt{k_B T} \sum_{\mathbf{G}\neq-\mathbf{q}} \left[ \frac{\hat{\mathbf{n}}\mathbf{h} : \hat{\mathbf{S}}_l}{c_{l\sqrt{\rho}}} + \frac{\hat{\mathbf{n}}\mathbf{h} : \hat{\mathbf{S}}_{t_1}}{c_{t_1\sqrt{\rho}}} + \frac{\hat{\mathbf{n}}\mathbf{h} : \hat{\mathbf{S}}_{t_2}}{c_{t_2\sqrt{\rho}}} \right] \frac{\left\langle m\mathbf{k}+\mathbf{q} \mid e^{i(\mathbf{q}+\mathbf{G})\cdot\mathbf{r}} \mid n\mathbf{k} \right\rangle}{\mid \mathbf{q}+\mathbf{G} \mid} \tag{S5}$$

where $\mathbf{h}$ is the full piezoelectric stress tensor and $\hat{\mathbf{n}} = (\mathbf{q}+\mathbf{G})/\mid \mathbf{q}+\mathbf{G} \mid$ is a unit vector in the direction of scattering.

The polar optical phonon differential scattering rate is given by

$$g_{nm}^{POP}(\mathbf{k},\mathbf{q}) = \left[ \frac{\hbar\omega_{po}}{2} \right]^{1/2} \sum_{\mathbf{G}\neq-\mathbf{q}} \left( \frac{1}{\hat{n}\cdot\epsilon_\infty\cdot\hat{n}} - \frac{1}{\hat{n}\cdot\epsilon_s\cdot\hat{n}} \right) \frac{\left\langle m\mathbf{k}+\mathbf{q} \mid e^{i(\mathbf{q}+\mathbf{G})\cdot\mathbf{r}} \mid n\mathbf{k} \right\rangle}{\mid \mathbf{q}+\mathbf{G} \mid} \tag{S6}$$

where $\epsilon_s$ and $\epsilon_\infty$ are the static and high-frequency dielectric tensors and $\omega_{po}$ is the polar optical phonon frequency. To capture scattering from the full phonon band structure in a single phonon frequency, each phonon mode is weighted by the dipole moment it produces.

The ionized impurity matrix element is given by

$$g_{nm}^{IMP}(\mathbf{k},\mathbf{q}) = \sum_{\mathbf{G}\neq-\mathbf{q}} \frac{n_{imp}^{1/2} Ze}{\hat{n}\cdot\epsilon_s\cdot\hat{n}} \frac{\left\langle m\mathbf{k}+\mathbf{q} \mid e^{i(\mathbf{q}+\mathbf{G})\cdot\mathbf{r}} \mid n\mathbf{k} \right\rangle}{\mid \mathbf{q}+\mathbf{G} \mid^2 + \beta^2} \tag{S7}$$

where $Z$ is the charge state of the impurity center, $n_{imp}$ is the concentration of ionized impurities (i.e., $C \times (n_{holes} - n_{electrons})/Z$ where $C$ is the amount of charge compensation), and $\beta$ is the inverse screening length, defined as

$$\beta^2 = \frac{e^2}{\epsilon_s \kappa_B T} \int \frac{\mathrm{d}\varepsilon}{V} D(\varepsilon) f(1-f) \tag{S8}$$

where $V$ is the unit cell volume, $D$ is the density of states, and $f$ is the Fermi–Dirac distribution given in the transport properties section.

The effective phonon frequency is determined from the phonon frequencies $\omega_{\mathbf{q}\nu}$ (where $\nu$ is a phonon branch and $\mathbf{q}$ is a phonon wave vector) and eigenvectors $\mathbf{e}_{\kappa\nu}(\mathbf{q})$ (where $\kappa$ is an

atom in the unit cell). In order to capture scattering from the full phonon band structure in a single phonon frequency, each phonon mode is weighted by the dipole moment it produces according to

$$\omega_\nu = \sum_\kappa \left[\frac{1}{M_\kappa \omega_{q\nu}}\right]^{1/2} \times [\mathbf{q} \cdot \mathbf{Z}^*_\kappa \cdot \mathbf{e}_{\kappa\nu}(\mathbf{q})] \tag{S9}$$

where $\mathbf{Z}^*_\kappa$ is the Born effective charge. This naturally suppresses the contributions from transverse-optical and acoustic modes in the same manner as the more general formalism for computing Frölich based electron-phonon coupling.

The weight is calculated only for Γ-point phonon frequencies and averaged over the full unit sphere to capture both the polar divergence at $\mathbf{q} \to 0$ and any anisotropy in the dipole moments. The effective phonon frequency is calculated as the weighted sum over all Γ-point phonon modes according to

$$\omega_{po} = \frac{\omega_{\Gamma\nu} w_\nu}{\sum_\nu w_\nu} \tag{S10}$$

Finally, we solve for the electronic BTE using the band gap value calculated by the HSE06 function as input. The following is a representation of the electron transport parameters tensor Seebeck coefficient(S), electrical conductivity($\sigma$), and electronic thermal conductivity($\kappa_e$)

$$S^{\alpha\beta} = \frac{\int \Sigma_{\alpha\beta}(\varepsilon)(\varepsilon - \varepsilon_F)\left[-\frac{\partial f^0}{\partial \varepsilon}\right] \mathrm{d}\varepsilon}{eT \int \Sigma_{\alpha\beta}(\varepsilon)\left[-\frac{\partial f^0}{\partial \varepsilon}\right] \mathrm{d}\varepsilon} \tag{S11}$$

$$\sigma^{\alpha\beta} = e^2 \int \Sigma_{\alpha\beta}(\varepsilon)\left[-\frac{\partial f^0}{\partial \varepsilon}\right] \mathrm{d}\varepsilon \tag{S12}$$

$$\kappa_e^{\alpha\beta} = \left\{ \frac{(\int \Sigma_{\alpha\beta}(\varepsilon)(\varepsilon - \varepsilon_F)\left[-\frac{\partial f^0}{\partial \varepsilon}\right])^2 d\varepsilon}{T \int \Sigma_{\alpha\beta}(\varepsilon)\left[-\frac{\partial f^0}{\partial \varepsilon}\right] \mathrm{d}\varepsilon} - \frac{1}{T} \int \Sigma_{\alpha\beta}(\varepsilon)(\varepsilon - \varepsilon_F)^2 \left[\frac{\partial f^0}{\partial \varepsilon}\right] \mathrm{d}\varepsilon \right\} \tag{S13}$$

Among them, e, T, $\varepsilon_F$, $\Sigma_{\alpha\beta}(\varepsilon)$ and $f^0$ are the electron charge, absolute temperature, certain doped Fermi level, spectral conductivity and Fermi-Dirac distribution function respectively. Spectral conductivity is defined as

$$\Sigma_{\alpha\beta}(\varepsilon) = \sum_n \int \frac{d\mathbf{k}}{8\pi^3} \upsilon^\alpha_{n\mathbf{k}} \upsilon^\beta_{n\mathbf{k}} \tau_{n\mathbf{k}} \delta(\varepsilon - \varepsilon_{n\mathbf{k}}) \tag{S14}$$

in which, n is the electron band index, $\mathbf{k}$ stands the wave vector, $\alpha$ and $\beta$ represent Cartesian coordinates, $\upsilon_{n\mathbf{k}}$ is the energy, $\upsilon^{\alpha(\beta)}_{n\mathbf{k}}$ denote the electron group velocity.

We give the deformation potential of these two materials calculated using AMSET software as follows:

(1) The Valence band maximum of $K_2RbSb$

band: 29-30

k-point: $\begin{bmatrix}0.00 & 0.00 & 0.00\end{bmatrix}$; deformation potential: $\begin{bmatrix}1.81 & 1.31 & 1.31\\ 1.31 & 1.81 & 1.31\\ 1.31 & 1.31 & 1.81\end{bmatrix}$

band: 31-32

k-point: $\begin{bmatrix}0.00 & 0.00 & 0.00\end{bmatrix}$; deformation potential: $\begin{bmatrix}1.80 & 1.37 & 1.37\\ 1.37 & 1.80 & 1.37\\ 1.37 & 1.37 & 1.80\end{bmatrix}$

(2) The Conduction band minimum of $K_2RbSb$

band: 33-34

k-point: $\begin{bmatrix}0.00 & 0.00 & 0.00\end{bmatrix}$; deformation potential: $\begin{bmatrix}2.01 & 0.03 & 0.03\\ 0.03 & 2.01 & 0.03\\ 0.03 & 0.03 & 2.01\end{bmatrix}$

(3) The Valence band maximum of $Rb_2KSb$

band: 31-32

k-point: $\begin{bmatrix}0.00 & 0.50 & 0.50\end{bmatrix}$; deformation potential: $\begin{bmatrix}1.90 & 0.00 & 0.00\\ 0.00 & 0.50 & 0.14\\ 0.00 & 0.14 & 0.50\end{bmatrix}$

(4) The Conduction band minimum of $Rb_2KSb$

band: 33-34

k-point: $\begin{bmatrix}0.00 & 0.00 & 0.00\end{bmatrix}$; deformation potential: $\begin{bmatrix}1.45 & 0.02 & 0.02\\ 0.02 & 1.45 & 0.02\\ 0.02 & 0.02 & 1.45\end{bmatrix}$

## B. Supplementary Figures and Tables.

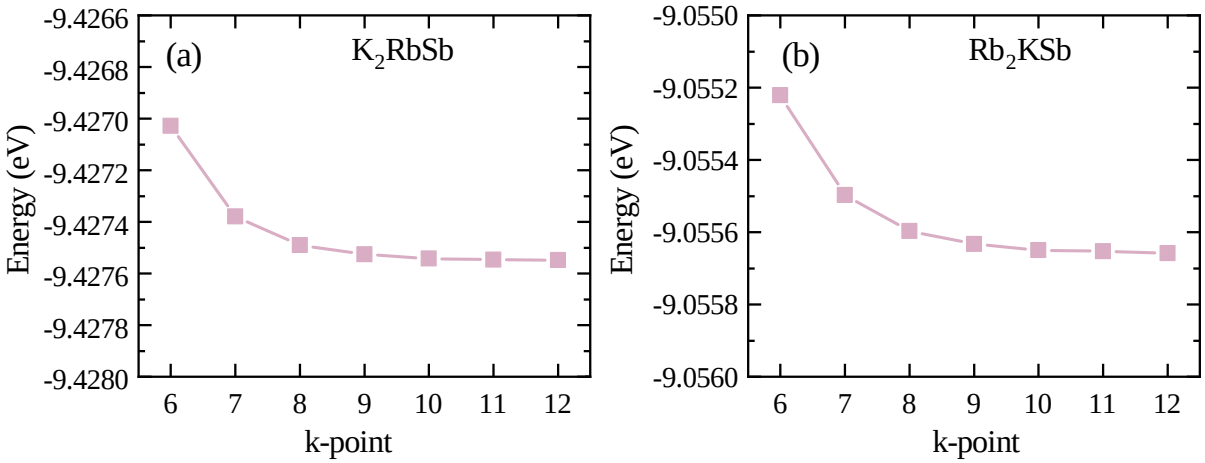


**Fig. S1**. (Color online). The k-point convergence test for (a) $K_2RbSb$ and (b) $Rb_2KSb$.

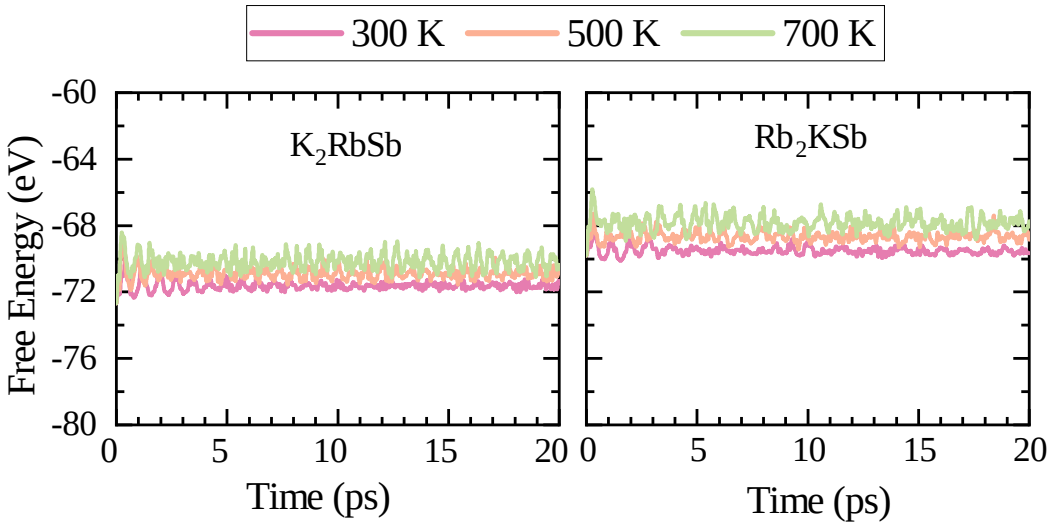


**Fig. S2**. (Color online). The AIMD simulations for (a) $K_2RbSb$ and (b) $Rb_2KSb$.

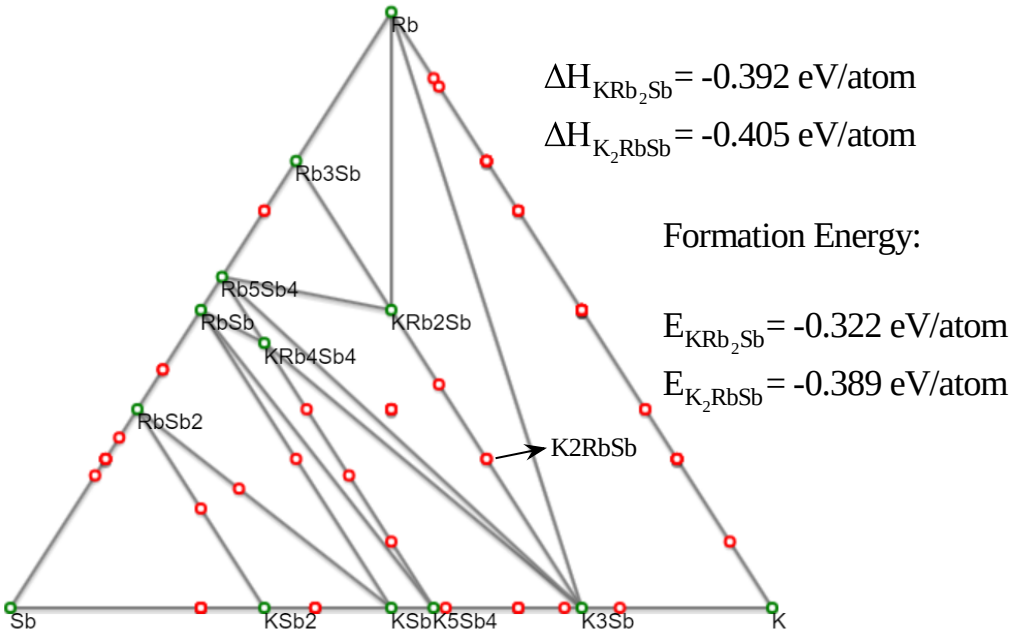


**Fig. S3**. (Color online). The phase diagram of K-Rb-Sb from the Open Quantum Materials Database (OQMD).

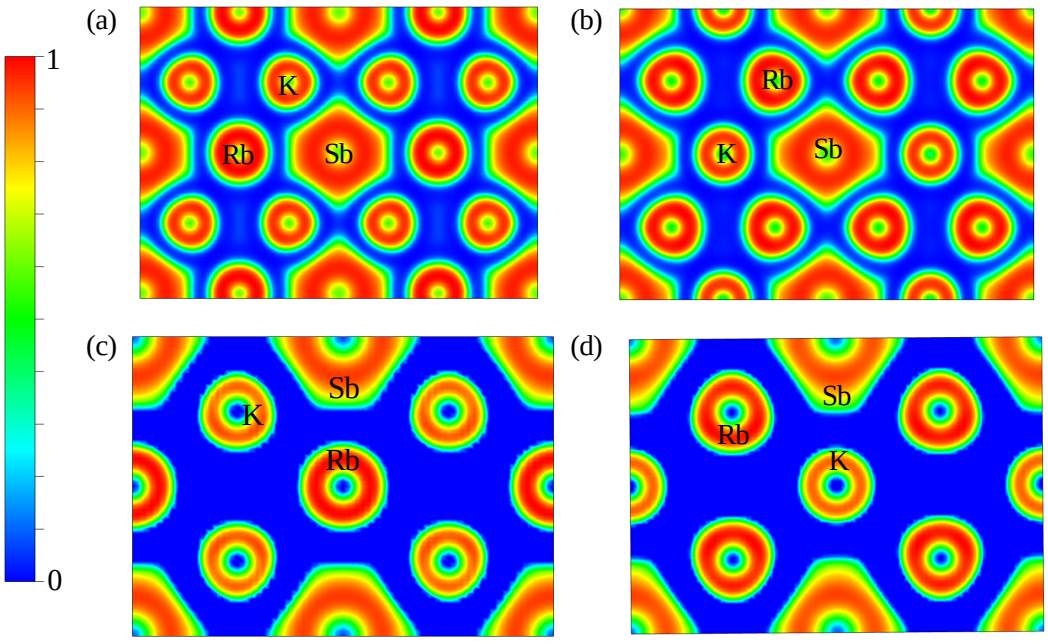


**Fig. S4**. (Color online). The 2D projected electron localization function (ELF) in (110) plane for (a) $K_2RbSb$ and (b) $Rb_2KSb$. The (011) plane of (c) $K_2RbSb$ and (d) $Rb_2KSb$, the distances from the origin are 6.01 Åand 6.10 Å

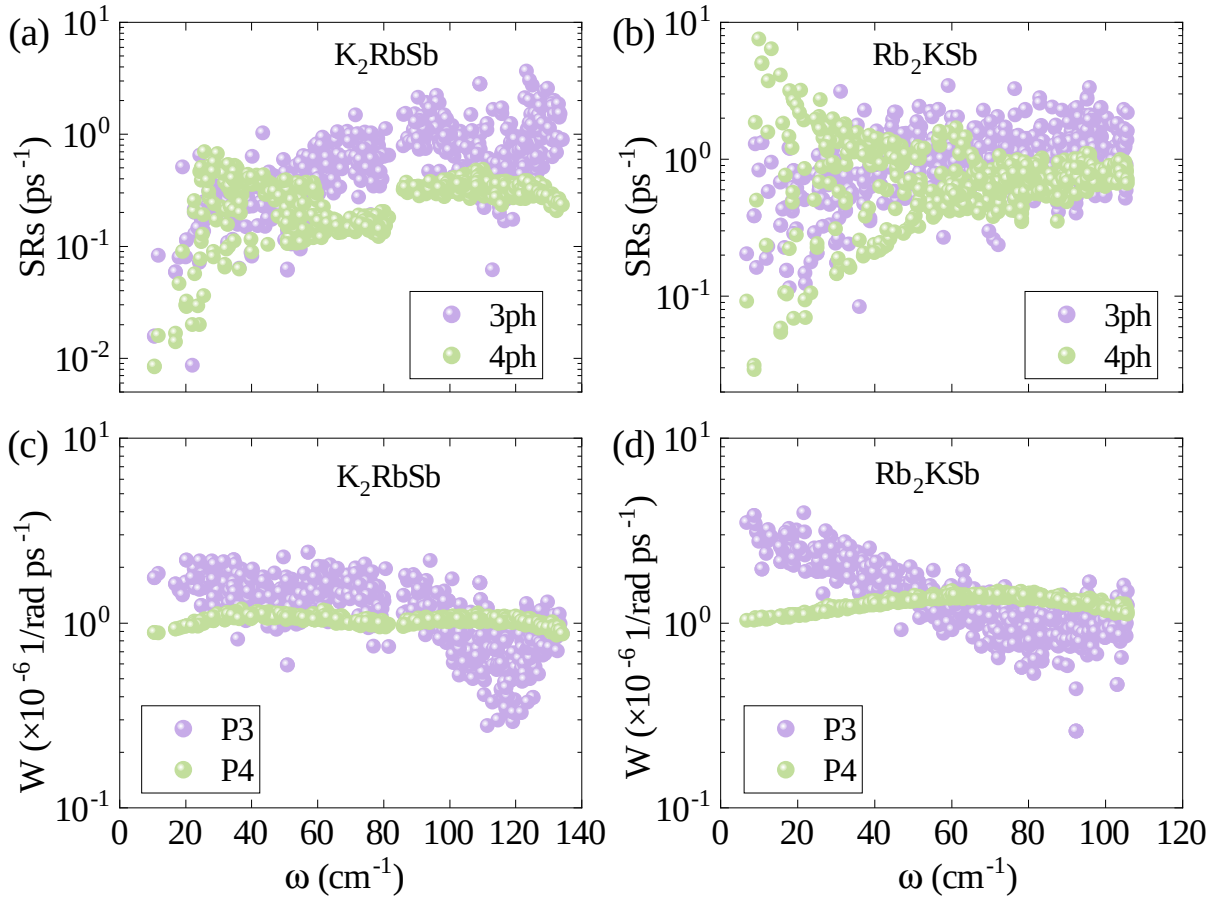


**Fig. S5**. (Color online). The scattering rate (SRs) and scattering phase space of 3ph and 4ph were calculated by SCP approximation at 300 K for $K_2RbSb$ and $Rb_2KSb$.

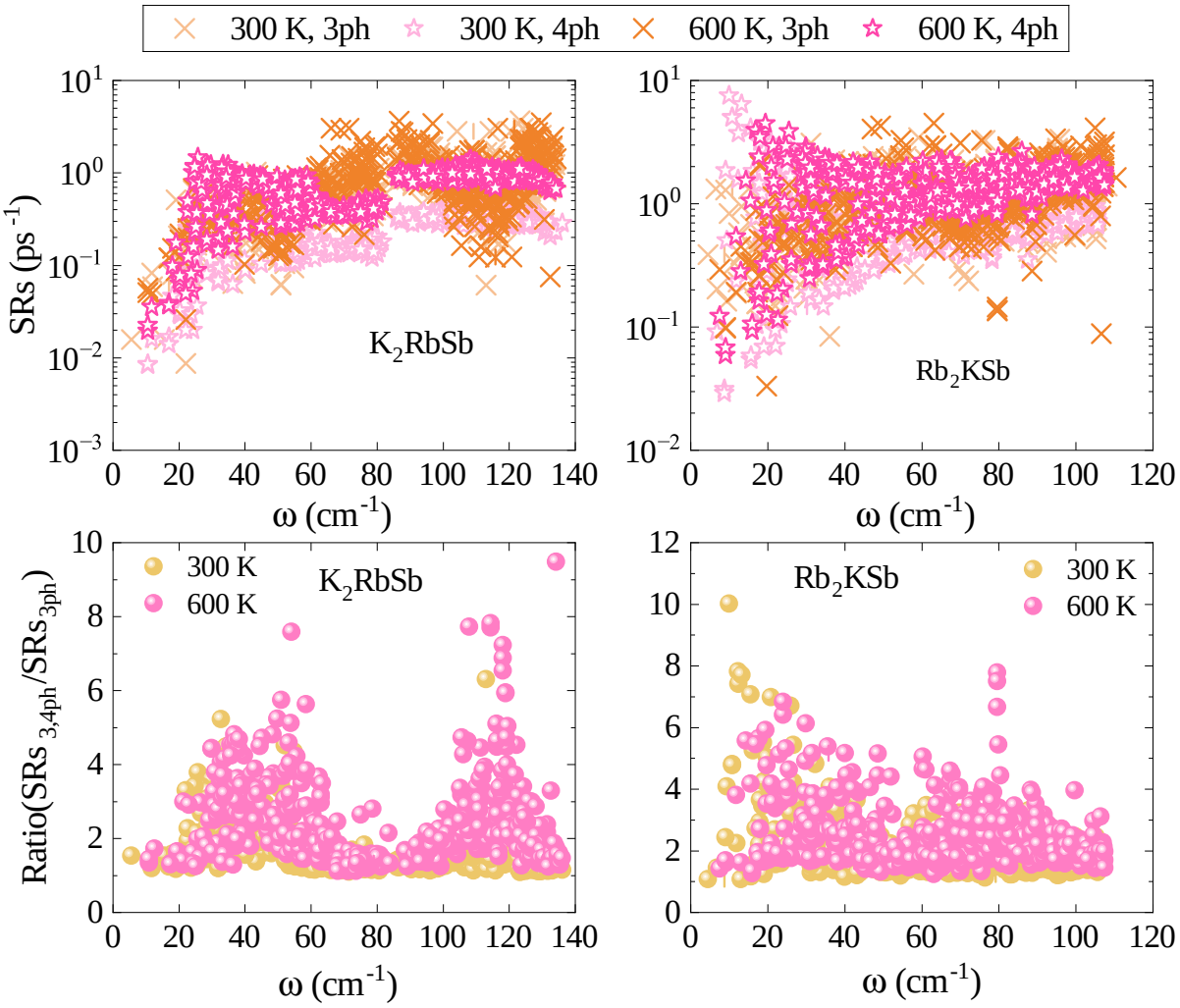


**Fig. S6**. (Color online). The scattering rate (SRs) of 3ph, 4ph and the ratio of SRs at 300 K and 600 K for $K_2RbSb$ and $Rb_2KSb$.

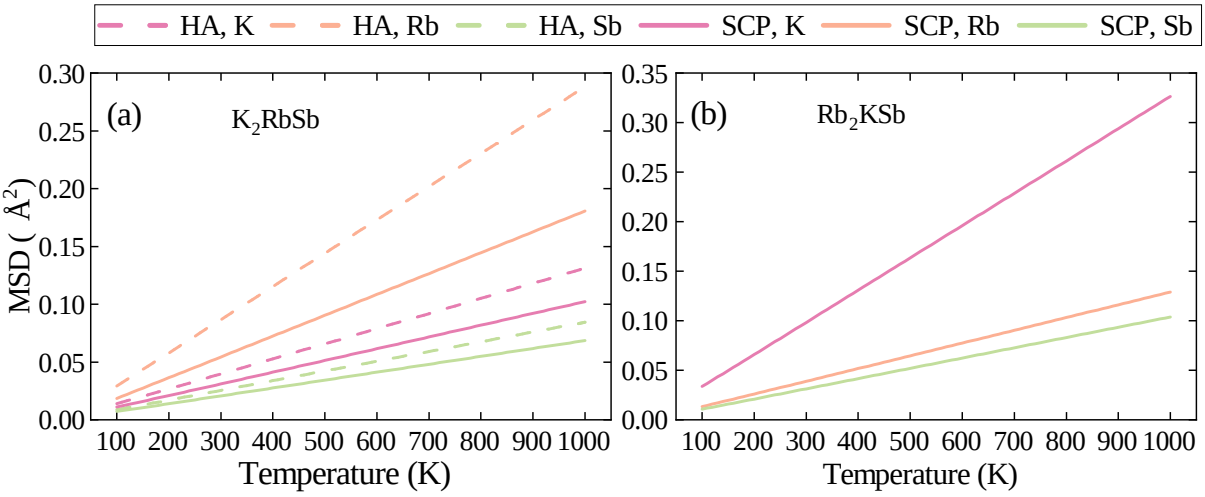

**Fig. S7**. (Color online). The temperature dependent atomic mean square displacements (MSD) of (a) $K_2RbSb$, and (b) $Rb_2KSb$ were calculated by HA and SCP method.

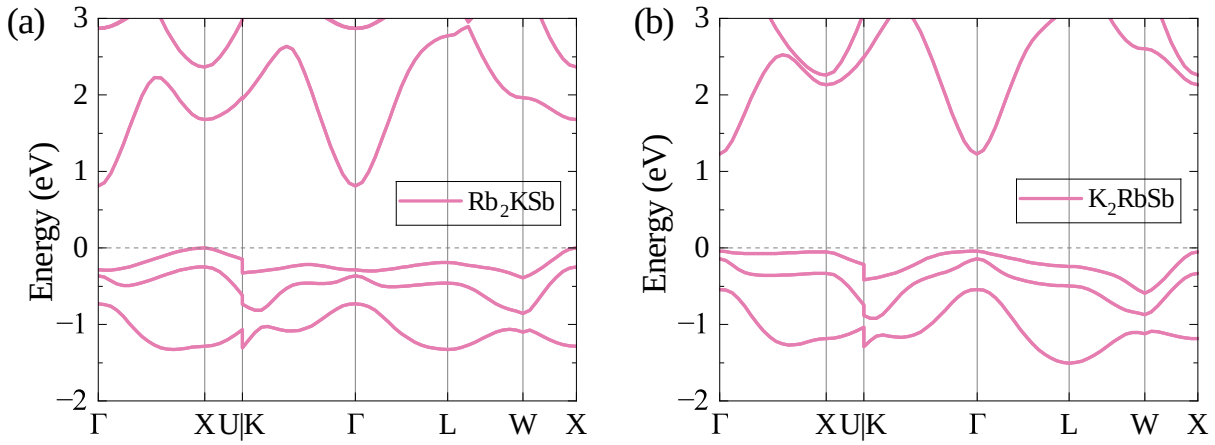


**Fig. S8**. (Color online). The electron band structure using HSE06 method with SOC for (a) $K_2RbSb$ and (b) $Rb_2KSb$.

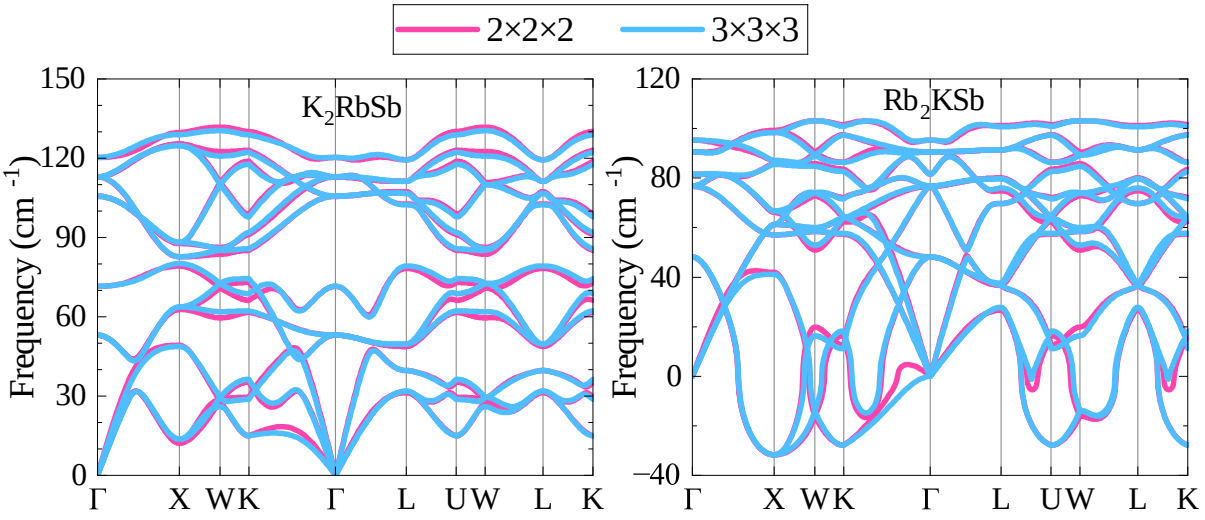


**Fig. S9**. (Color online). The comparison of harmonic phonon dispersion between different supercells of $K_2RbSb$ and $Rb_2KSb$.

TABLE S1. Born Effective Charge (Z*)

| | K | Rb | Sb |
|---|---|---|---|
| $RbK_2Sb$ | 0.8558 | 1.2121 | -2.9236 |
| $Rb_2KSb$ | 1.3955 | 0.7461 | -2.8878 |

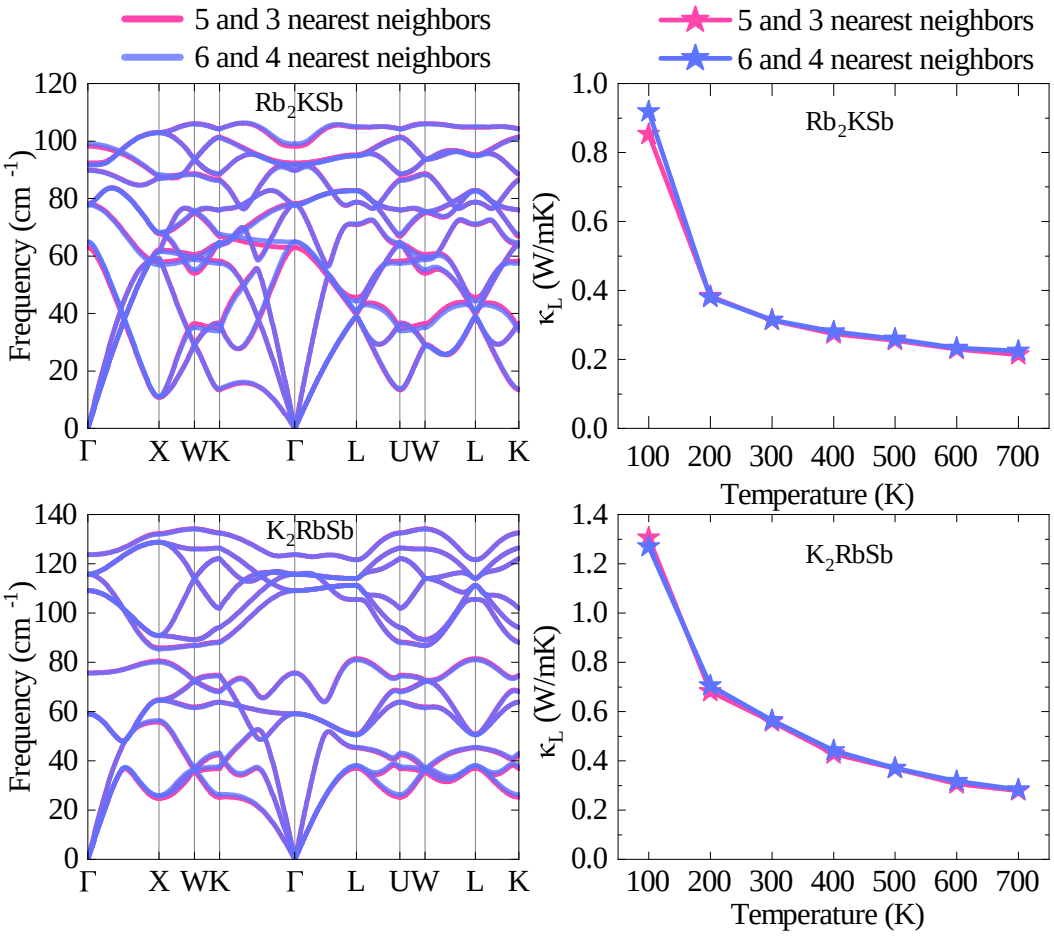


**Fig. S10**. (Color online). The phonon spectra at 300 K and lattice thermal conductivity of $Rb_2KSb$ and $K_2RbSb$ obtained based on the high-order force constants extracted at different cutoff radius.


* y.zhao@ytu.edu.cn

† zhdai@ytu.edu.cn

TABLE S2. The lattice thermal conductivity and its coherent term.

| material | $RbK_2Sb$ | | | $Rb_2KSb$ | | |
|---|---|---|---|---|---|---|
| T | $\kappa_L^{coherent}$ | $\kappa_L$ | $\kappa_L^{coherent}/\kappa_L^{Total}$ | $\kappa_L^{coherent}$ | $\kappa_L$ | $\kappa_L^{coherent}/\kappa_L^{Total}$ |
| 100 K | 0.0060 | 1.3057 | 0.0045 | 0.1177 | 0.8528 | 0.1213 |
| 200 K | 0.0103 | 0.6809 | 0.0149 | 0.0516 | 0.3823 | 0.1189 |
| 300 K | 0.0131 | 0.5592 | 0.0228 | 0.0480 | 0.3129 | 0.1330 |
| 400 K | 0.0145 | 0.4287 | 0.0327 | 0.0418 | 0.2744 | 0.1322 |
| 500 K | 0.0158 | 0.3696 | 0.0409 | 0.0389 | 0.2548 | 0.1324 |
| 600 K | 0.0166 | 0.3072 | 0.0512 | 0.0379 | 0.2299 | 0.1415 |

TABLE S3. The band effective masses ($m^*$).

| material | $RbK_2Sb$ | | | $Rb_2KSb$ | | | |
|---|---|---|---|---|---|---|---|
| K-Path | $\Gamma \rightarrow K$ | $\Gamma \rightarrow L$ | $\Gamma \rightarrow X$ | $X \rightarrow \Gamma$ | $X \rightarrow U$ | $\Gamma \rightarrow K$ | $\Gamma \rightarrow L$ |
| Hole(VBM) | -9.313$m_0$ | -2.475$m_0$ | -13.489$m_0$ | -3.929$m_0$ | -3.333$m_0$ | | |
| Electron(CBM) | 0.182$m_0$ | 0.178$m_0$ | 0.192$m_0$ | | | 0.179$m_0$ | 0.178$m_0$ |